

Neutron spectroscopy within the $S=5$ ground multiplet and low-temperature heat capacity in an Fe_4 magnetic cluster

G. Amoretti and S. Carretta

Istituto Nazionale per la Fisica della Materia, Dipartimento di Fisica, Università di Parma, Parco Area delle Scienze 7/A, I-43100 Parma, Italy

R. Caciuffo

Istituto Nazionale per la Fisica della Materia, Dipartimento di Fisica e Ingegneria dei Materiali e del Territorio, Università di Ancona, Via Breccie Bianche, I-60131 Ancona, Italy

H. Casalta

Institut Laue-Langevin, 6 rue Horowitz, F-38042 Grenoble, France

A. Cornia

Dipartimento di Chimica, Università di Modena e Reggio Emilia, Via Campi 183, I-41100 Modena, Italy

M. Affronte

Istituto Nazionale per la Fisica della Materia, Dipartimento di Fisica, Università di Modena e Reggio Emilia, Via Campi 213/a, I-41100 Modena, Italy

D. Gatteschi

Dipartimento di Chimica, Università di Firenze, Via Maragliano 77, I-50144 Firenze, Italy

(Received 27 April 2001; published 7 August 2001)

The transitions within the $S=5$ ground state of the tetrairon(III) molecular cluster $\text{Fe}_4(\text{OCH}_3)_6(\text{dpm})_6$ (Hdpm = dipivaloylmethane) have been measured by inelastic neutron scattering. The spectra have been interpreted by means of an effective spin Hamiltonian for an isolated $S=5$ multiplet, taking into account the presence of three different isomers in the compound. It has been shown that for the two dominant isomers the symmetry of the zero-field splitting tensor is not purely axial, but a nonzero rhombic coefficient E is needed to fit the neutron spectra. The results have been discussed in comparison with recent high-field electron paramagnetic resonance data in single crystals. Heat-capacity measurements in the range 2 to 20 K have been performed and shown to be compatible with the neutron results for the zero-field splitting.

DOI: 10.1103/PhysRevB.64.104403

PACS number(s): 75.50.Tt, 75.10.Jm, 75.40.Gb, 75.45.+j

I. INTRODUCTION

The magnetic properties of metal ion clusters separated by shells of organic ligand molecules are drawing increasing attention, both for the physics involved and for the potential applications they promise.¹ At low temperatures, these molecules act as individual, identical, quantum nanomagnets, enabling to probe, at the macroscopic scale, the crossover between quantum and classical physics.² Of fundamental interest are the quantum-size effects on the thermodynamic properties³ and the situation of near degeneracy of two magnetic levels, where quantum phenomena such as tunneling or coherence can occur. These effects have been explored in the high-spin molecules Mn_{12} and Fe_8 ,^{4,5} two systems characterized by a peculiar steplike magnetic hysteresis cycle, and a very slow relaxation of the magnetization at low temperature. The interesting behavior is associated with the zero-field splitting (ZFS) of the spin ground state and with the Ising-type energy barrier to be overcome for the reversal of the magnetic moment.

It has been recently shown that inelastic neutron scattering (INS) can provide unique information on the ZFS in molecular clusters of magnetic transition-metal ions. The

first application of INS to the determination of the anisotropy splitting of the ground state in a magnetic cluster was to the compound $[\text{Fe}_8\text{O}_2(\text{OH})_{12}(\text{tacn})_6]\text{Br}_8$ (briefly Fe_8), where *tacn* is the organic ligand triazacyclononane.⁶ This system is constituted by weakly interacting molecular clusters of eight iron(III) ions, characterized by an overall D_2 symmetry and by a magnetic ground state with an effective spin $S=10$. The INS experiment was performed on the time-of-flight spectrometer IN5 at the Institute Laue-Langevin in Grenoble and it allowed the accurate determination of the ZFS parameters, up to fourth order, of the anisotropic spin Hamiltonian of the cluster from the analysis of the transitions within the ground multiplet.

In the case of $[\text{Mn}_{12}\text{O}_{12}(\text{CH}_3\text{COO})_{16}(\text{H}_2\text{O})_4]$ (briefly Mn_{12}),^{7,8} the symmetry is tetragonal and the spectrum is more simple than that of Fe_8 , which is characterized by considerable mixing of the $|SM\rangle$ components of the $S=10$ multiplet, particularly for $|M|\leq 6$.

It has been shown also that the role of higher-order parameters may be crucial to determine some details of the neutron spectra related to transitions between strongly mixed wave functions, which are populated at sufficiently high temperature. In some cases, high-resolution experiments are needed in order to determine directly these ZFS parameters,

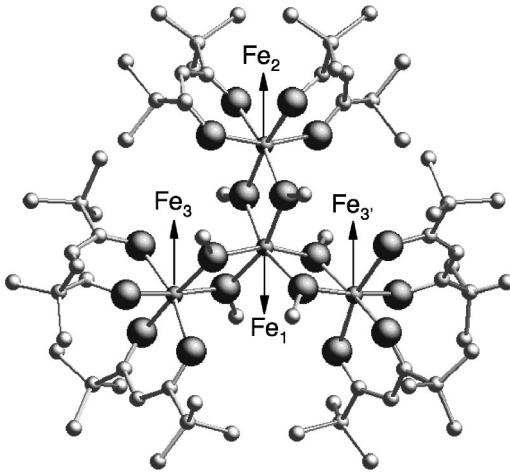


FIG. 1. Schematic molecular structure of the Fe_4 cluster. Large black and small gray circles are oxygen ions and carbon atoms, respectively. The Fe(III) ions are represented by small black circles. Hydrogen atoms are not shown for clarity. Arrows indicate the Fe magnetic moments.

which by high-field electron paramagnetic resonance (HF-EPR) can only be extrapolated from the asymptotic magnetic-field region.⁹

We have performed the neutron spectroscopy study of a tetrairon(III) cluster of formula $\text{Fe}_4(\text{OCH}_3)_6(\text{dpm})_6$ (Hdpm = dipivaloylmethane), which has an $S=5$ ground state and shows slow relaxation of the magnetization below 1 K.¹⁰ The molecular structure of this cluster (briefly called Fe_4), is shown in Fig. 1. The four iron atoms lie exactly in a plane, the inner Fe atom being in the center of an isosceles triangle. The molecule has a twofold symmetry due to the presence of a crystallographic C_2 axis passing through Fe1 and Fe2. The intramolecular Fe \cdots Fe distances are 3.146(2) Å and 3.133(1) Å for the pairs Fe1-Fe2 and Fe1-Fe3, respectively. The edges of the iron triangle take the values of 5.372(2) Å (Fe2-Fe3 and Fe2-Fe3') and 5.550(2) Å (Fe3-Fe3'), while $2\hat{1}3$ and $3\hat{1}3'$ angles are $117.65(3)^\circ$ and $124.70(6)^\circ$, respectively.

HF-EPR spectroscopy on a powder sample revealed that the system has an essentially uniaxial magnetic anisotropy with $D = -0.20 \text{ cm}^{-1} = -24.8 \text{ } \mu\text{eV}$. The sign of D and the unresolved rhombicity of the spectra are consistent with the expected single-ion anisotropies based on the angular overlap model and with the estimated intramolecular dipole-dipole contributions, although the calculated absolute value of D is only 30% of the experimental value. The theoretical analysis in Ref. 10 also indicated that the unique axis of the \mathbf{D} tensor is likely to be almost parallel to the pseudo- C_3 axis of the molecule (perpendicular to the plane of the four iron atoms).

The INS measurements herein reported are in line with this hypothesis and provide the complete pattern of zero-field energy levels in Fe_4 . This depends sensitively on the rhombic coefficient E in the anisotropy spin Hamiltonian describing splitting of the ground state.

After our experiment was performed and during the analysis of the data, single-crystal HF-EPR results became

available,¹² which will be compared with ours and discussed below. The presence of three different structural variations of the compound, already found by x-ray analysis,¹⁰ was confirmed by the EPR measurements and will be taken into account for the interpretation of the INS spectra. We will also show that a nonzero value of the rhombic term in the spin Hamiltonian for both the dominant isomers is needed to obtain a good fitting of the neutron data.

Heat-capacity measurements in the temperature range 2 to 20 K will also be presented and discussed in the frame of the neutron results for the ZFS.

II. NEUTRON RESULTS

The INS experiment was performed with the high-energy resolution multichopper time-of-flight spectrometer IN5, at the Institute Laue-Langevin, in Grenoble, France.

Due to the large number of hydrogen atoms in Fe_4 , a 98%-deuterated microcrystalline sample was used. The synthesis of $d_{18}\text{-Hdpm}$ (98 atom% D) will be reported elsewhere.¹¹ Pure Fe_4 was synthesized by following the original procedure¹⁰ with only minor modifications to reduce the volume of CD_3OD employed (99.8 atom% D). All operations were carried out with strict exclusion of moisture under a N_2 atmosphere. A 5.4-M solution of NaOCD_3 was prepared by careful addition of metallic Na (1.24 g, 54 mmol) to CD_3OD (10 mL). Resublimated FeCl_3 (0.812 g, 5.0 mmol) and $d_{18}\text{-Hdpm}$ (1.012 g, 5.0 mmol) were dissolved in CD_3OD (30 mL). NaOCD_3 (2.6 mL, 14.0 mmol) was added dropwise to the resulting deep red solution to give a yellow slurry, which was treated with an additional 20 mL of CD_3OD and stirred for ten minutes. Freshly distilled diethylether (100 mL) was then added and the undissolved NaCl was removed by centrifugation. Slow diffusion of CD_3OD vapors into the clear orange-yellow solution afforded yellow rodlike crystals of Fe_4 in 1 week. The crystals were isolated by filtration, washed with CD_3OD , and dried under vacuum (0.6 g, 45%-yield based on $d_{18}\text{-Hdpm}$). The degree of deuteration was checked by mass spectroscopy and ^1H nuclear magnetic resonance. Single-crystal EPR spectra at 95 GHz were identical to those reported in Ref. 12.

Two grams of the sample were encapsulated in an aluminum can and put into a standard liquid-He cryostat. Data were collected at different temperatures between 1 and 10 K, with an incident neutron energy of 1.01 meV, giving a resolution of $19 \text{ } \mu\text{eV}$ at the elastic peak position. The usual data treatment procedure was followed to correct the data for absorption and detector efficiency; normalization runs were collected on a vanadium standard and the background was determined from an empty-can run. A constant background was subtracted from the measured intensity before time-of-flight to energy conversion.

The spectra obtained at 1.7 and 6.5 K are shown in Fig. 2. The main inelastic peak at the highest positive energy at 1.7 K corresponds (assuming a purely axial anisotropy) to the transition between the ground $|S=5; M=\pm 5\rangle$ and the first excited $|S=5; M=\pm 4\rangle$ states of the split $S=5$ multiplet. Due to the quite small splitting between these two levels (about 2.5 K), at the temperature of the experiment the ex-

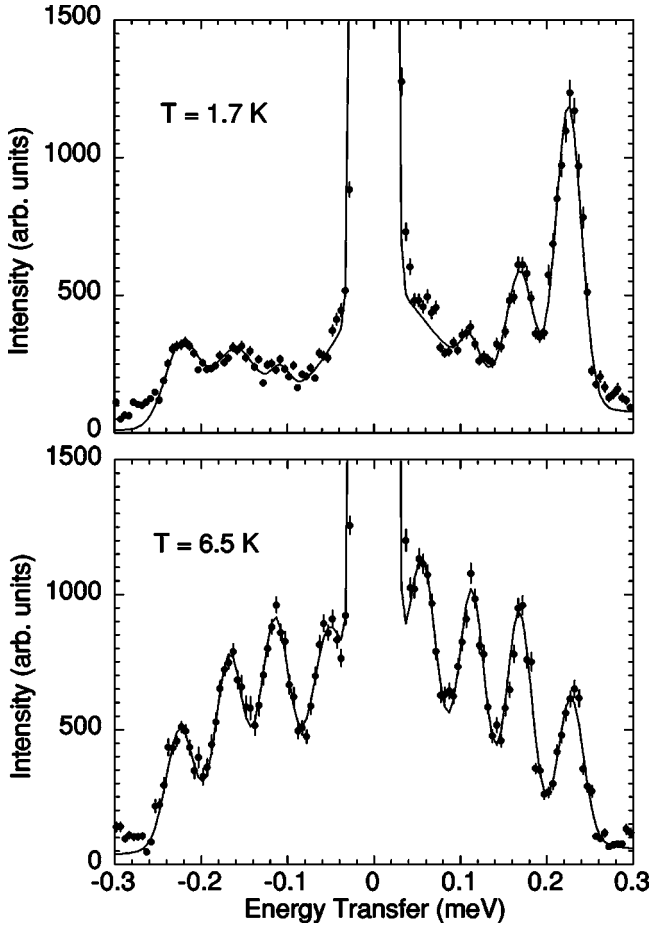


FIG. 2. The experimental INS spectrum at 1.7 and 6.5 K. The incident energy is 1.01 meV and the resolution 0.019 meV at the elastic peak. The empty-can signal has been subtracted.

cited states start to become populated and the transitions $|M = \pm 4\rangle \rightarrow |M = \pm 3\rangle$ and $|M = \pm 3\rangle \rightarrow |M = \pm 2\rangle$ are clearly visible. At lowest energy the shoulder on the elastic peak is due to the transition $|M = \pm 2\rangle \rightarrow |M = \pm 1\rangle$. As we will discuss in the following, the assumption of axial anisotropy is not adequate to interpret the neutron results; the true eigenstates are mixtures of the axial $|\pm M\rangle$ components and the above description is only approximate. It must be noted that the full width at half maximum (FWHM) deduced from the main peak is $33 \mu\text{eV}$, hence larger than the resolution. This is indicative of the intrinsic inhomogeneity of the compound, as described in Refs. 10 and 12.

In the spectrum recorded at 6.5 K, all the transitions between excited states are well developed. Because of the presence of different isomers, they are grouped together in well-separated peaks of width larger than the resolution.

III. THE SPIN HAMILTONIAN

The interpretation of the INS results is based on the hypothesis that the system can be described as an effective $S=5$ multiplet in presence of a crystal-field-like potential giving rise to the anisotropy. Since the overall splitting of the ground multiplet is of the order of 7 K, the effect of the

excited multiplets, which are 86-K higher in energy, can be neglected.

We assume a spin Hamiltonian up to fourth order of the type

$$H_S = \sum_{n,m} B_n^m \hat{O}_n^m, \quad (1)$$

with $n=2$ and 4 ($m = -n, \dots, n$). \hat{O}_n^m are Stevens operator equivalents¹³ defined in the space of the $S=5$ multiplet.

In the hypothesis that the system has essentially C_3 (or approximately D_3) symmetry with the threefold axis identified with the pseudo- C_3 axis, the spin Hamiltonian would be written

$$H_S = B_2^0 \hat{O}_2^0 + B_4^0 \hat{O}_4^0 + B_4^3 \hat{O}_4^3 + B_4^{-3} \hat{O}_4^{-3}, \quad (2)$$

where the last term is zero for D_3 symmetry, but in any case can be suppressed by a suitable rotation of the reference frame. The only nonvanishing second-order term in Eq. (2) is $B_2^0 \hat{O}_2^0$, where $B_2^0 = D/3$.¹⁴ Thus, up to this order the Hamiltonian is the same as that used for the simulation of the HF-EPR powder spectra in the purely axial assumption.¹⁰ However, this hypothesis is too poor to account for both the EPR spectra in single crystals (at least as regards one of the two dominant isomers)¹² and for the INS results.

In fact, the simulation of the INS spectra can be improved considerably if rhombic terms are added to the spin Hamiltonian. This assumption is compatible with both the hypotheses: (a) the system has a dominant axial symmetry along the pseudo- C_3 axis perpendicular to the iron plane and the rhombic contribution in the plane is due to the lack of exact threefold symmetry, the iron triangle being not equilateral. In this case a C_{1h} (i.e., σ_h) symmetry could be assumed to describe the leading contributions to the crystal field; (b) the cluster has a C_2 (or approximately C_{2v}) symmetry, with the twofold axis coincident with the C_2 axis of the molecule (i.e., the line from the vertex Fe2, perpendicular to the basis Fe3-Fe3' of the isosceles triangle in Fig. 1).

The spin Hamiltonian would be in both cases

$$H_S = B_2^0 \hat{O}_2^0 + B_2^2 \hat{O}_2^2 + B_4^0 \hat{O}_4^0 + B_4^2 \hat{O}_4^2 + B_4^4 \hat{O}_4^4 + B_4^{-2} \hat{O}_4^{-2} + B_4^{-4} \hat{O}_4^{-4}. \quad (3)$$

A term $B_2^{-2} \hat{O}_2^{-2}$ could be present in principle, but can be always eliminated by a reference frame rotation. Note that B_2^2 coincides with E in the usual notation for the ZFS second-order tensor.^{6,10} In the hypothesis (b), which however seems to be excluded by single-crystal EPR results, we would expect that the contribution of the $m < 0$ terms to the ZFS are negligible, since they are exactly zero in the assumption of C_{2v} symmetry.

IV. INTERPRETATION OF THE NEUTRON RESULTS AND DISCUSSION

The simulation of the INS spectra was performed by calculating, for each isomer, the transition energies for a given

TABLE I. The ZFS parameters (in μeV) used to simulate the neutron spectra (INS) for the three different isomers of Fe_4 , whose populations are fixed to the values given in parentheses. For convenience, the parameters given in Ref. 12 (EPR), in μeV units and with the notation of Eq. (1), are listed too.

Isomers	AA (49%)	AB (42%)	BB (9%)
INS			
B_2^0	-8.43 ± 0.06	-7.87 ± 0.06	-7.23
B_2^2	-2.5 ± 0.2	-1.1 ± 0.2	
$10^3 B_4^0$	-1.5 ± 0.3	-1.2 ± 0.3	-2.0
EPR			
B_2^0	-8.52 ± 0.04	-7.85 ± 0.07	-7.23 ± 0.07
B_2^2	-1.2 ± 0.4		
$10^3 B_4^0$	-1.4 ± 0.25	-2.0 ± 0.25	-2.0 ± 0.25
$10^2 B_4^2$	-1.0 ± 0.4		
$10^3 B_4^4$	-5.0 ± 4.0		

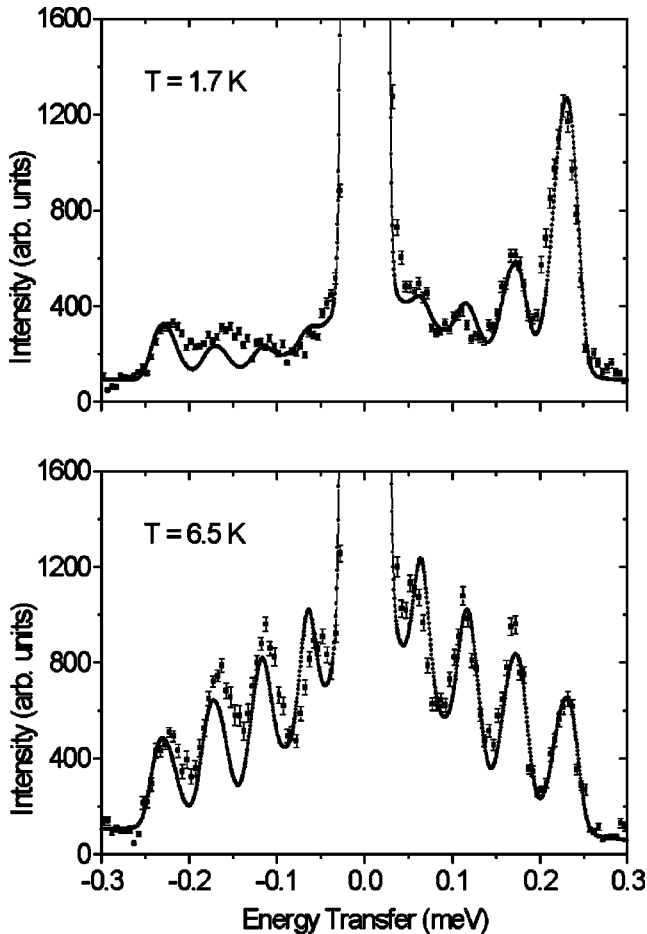


FIG. 3. Comparison between the experimental (squares) and the simulated INS spectrum (dash-dotted line) at 1.7 and 6.5 K, obtained by using the ZFS parameters from HF-EPR in single crystals (Ref. 12).

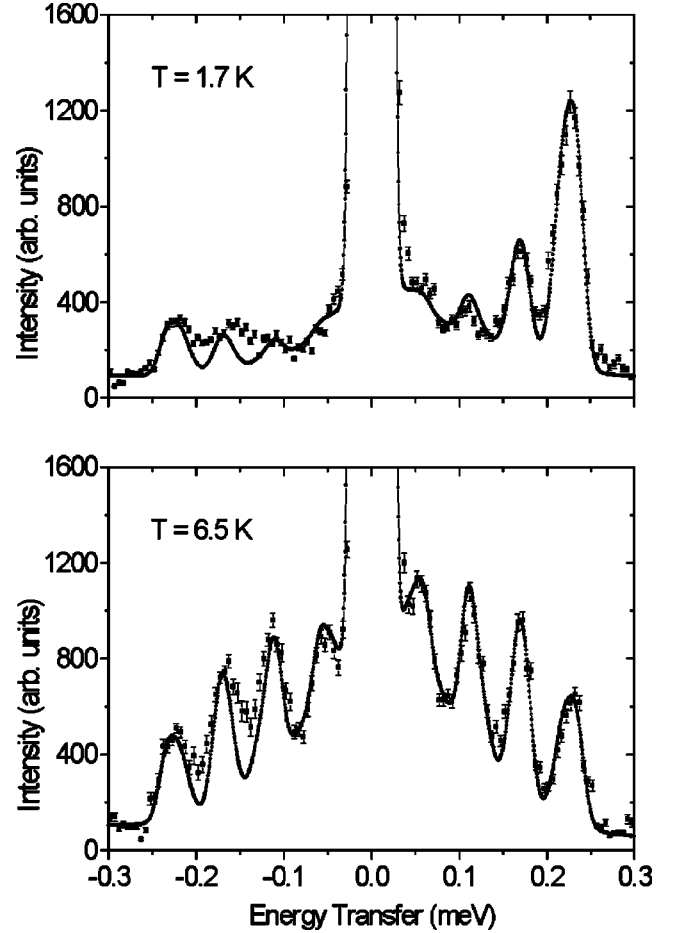


FIG. 4. Best fit of the experimental INS spectrum (squares) at 1.7 and 6.5 K. The simulated spectrum (dash-dotted line) is obtained using the parameters given in Table I (INS).

set of B_n^m parameters. To each transition we associated a Gaussian line shape with a height proportional to the transition probability and a width fixed to a value close to the instrument resolution of $19 \mu\text{eV}$. A FWHM of $21 \mu\text{eV}$ was shown to give the best results. We assumed for the populations of the three isomers, AA, AB and BB, whose structural differences were discussed in Ref. 12, the expected values 49%, 42% and 9%, respectively. The elastic peak and a quasielastic contribution, together with a sloping background, obtained by the best fit of the experimental spectrum, were added to the calculated inelastic contribution, properly normalized.

As a first attempt, we used the parameters determined by HF-EPR in the single crystals, which for convenience are reported in Table I. (EPR), with the notation of Eq. (1). The simulated spectra are shown in Fig. 3 for the two temperatures of 1.7 and 6.5 K. Although qualitatively good, the fitting is not satisfactory. Clearly, it is better at 1.7 than at 6.5 K, where the effect of the population of the excited states is more important and the spectrum more complex. In order to improve the agreement, we first varied the second-order parameters and the diagonal fourth-order parameter B_4^0 , allowing for a nonzero B_2^2 coefficient even for the AB isomer. Since the BB isomer is minor, its contribution is less critical.

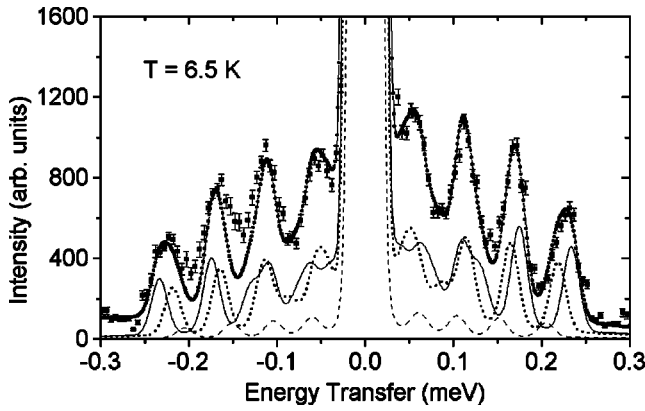


FIG. 5. The contributions of the different isomers to the simulated spectrum giving the best fit (dash-dotted line) of the experimental spectrum (squares) at 6.5 K: AA isomer, continuous line; AB, dotted line; BB, dashed line.

For simplicity we assumed for it the same spin Hamiltonian parameters as in Ref. 12. It was immediately seen that B_2^2 , i.e., E , for the AB isomer, must not be zero in order to significantly improve the fitting. In particular, if we try to vary all the parameters within the error bars given in Ref. 12, a satisfactory fitting is obtained with a value of E for the second isomer (AB) of about half that of the first one (AA).

However, a further significant improvement is achieved by using the parameters given in Table I. (INS). Within the

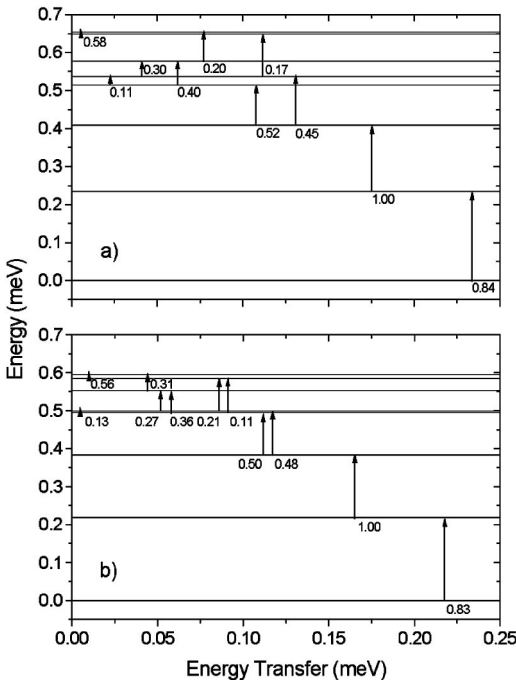


FIG. 6. Zero-field splitting of the $S=5$ ground-state multiplet and allowed transitions for the two dominant isomers of Fe_4 : (a) AA isomer; (b) AB isomers. Thicker horizontal lines correspond to doubly degenerate levels (within $4 \mu\text{eV}$). The main transitions in the dipole approximation are indicated by arrows, positioned at the corresponding energy transfer along the horizontal axis. The transition probabilities are also given close to each arrow.

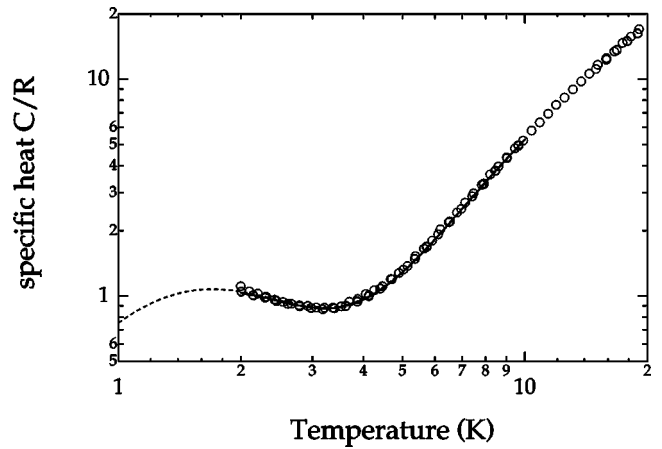


FIG. 7. Molar specific heat of Fe_4 measured in the temperature range 2 to 20 K and normalized to the gas constant R (circles). The continuous line represents the best fit as described in the text. The dashed line is the extrapolation of this curve to low temperature.

error bars, B_2^0 and B_4^0 have practically the same values deduced by fitting the EPR spectra. On the contrary, B_2^2 is twice the EPR value for AA, while for AB it is nonzero and about half the value of the first isomer.

The results are shown in Fig. 4 for low and high temperature. The fitting is good, particularly in the neutron energy-loss part of the spectrum ($\hbar\omega > 0$). As a general criterion for the fitting, we chose to weigh more the energy loss with respect to the energy-gain region of the spectrum, where some extra intensity is probably due to spurious signals. The error bars in Table I were estimated by considering simultaneous variations of all the parameters which do not affect appreciably the quality of the fitting.

As regards the off-diagonal fourth-order terms in Hamiltonian (3), the sensitivity of the present INS experiment is not sufficient to determine reliable values for their coefficients. This is due to the presence of the three different isomers, whose separate contributions to the simulated spectrum at 6.5 K are shown in Fig. 5.

Information on the higher-order parameters may be obtained from the analysis of details of the spectra, particularly at low exchanged energy. In fact, they contribute to mix the different $|SM\rangle$ components in the eigenfunctions, principally for $|M| \leq 3$, and give rise also to slight shifts of the levels. As a consequence, they affect the positions and the intensities of the numerous transitions between excited states appearing in the energy region below ~ 0.130 meV (see Fig. 6). Even in the case of a single isomer, these transitions may be very close to one another and grouped together to give apparently a single peak (as in the case of the peaks at about 0.11 and 0.05 meV), or also isolated and embedded in the elastic peak (corresponding to single transitions between very close levels). Therefore, very high resolution and/or very low-energy transfer is needed to assess more precise values for these parameters.⁹

To check the effect of the off-diagonal parameters on the calculated spectra, we have varied them (with various combination of the signs) around the values given in Ref. 12 for B_4^2 and B_4^4 , in the case of the AA isomer (see Table I). We

have found that the simulated spectra are affected by these parameters (particularly as regards the shape of the lowest-energy peak) only for values greater than about 10^{-2} μeV . However, the fitting tends to become worse and cannot be improved by further increasing the absolute values of the parameters. The negative m coefficients have in general a smaller effect than the $m > 0$ ones. Based on the actual INS data, we can therefore only indicate the above value as an upper limit for the off-diagonal terms.

V. HEAT-CAPACITY MEASUREMENTS

Nondeuterated microcrystals of Fe_4 , synthesized as reported in Ref. 10, were pressed, without any additive, in order to obtain a 6.6-mg compact specimen. Low-temperature heat capacity measurements were performed by using the relaxation method in a 7-T physical property measurement system of Quantum Design. The molar specific heat C of Fe_4 measured in the temperature range 2 to 20 K and normalized to the gas constant R is reported in Fig. 7. Due to the large number of atoms per molecule, the specific heat is dominated by a phonon contribution above 10 K, yet in the case of Fe_4 the magnetic Schottky anomaly turns out to be evident below 4 K. The continuous line in Fig. 7 is the fitting curve of data between 2 and 10 K. The dashed line is the extrapolation of this curve to low temperature, showing the expected behavior of the Schottky peak. For the data fitting we consider two contributions to the specific heat: $C = C_{ph} + C_{magn}$. We consider a lattice contribution C_{ph} (in R units) of the form

$$\frac{234rT^3}{(\Theta_D + \epsilon T^2)^3}, \quad (4)$$

where r is the number of atoms per molecule and ϵ accounts for the temperature dependence of Θ_D .¹⁵ The magnetic term $C_{magn}/R\beta^2$ (with $\beta^{-1} = k_B T$) of a system having a set of energy levels E_i can be expressed as

$$\frac{\sum_i E_i^2 \exp(-\beta E_i) \sum_i \exp(-\beta E_i) - [\sum_i E_i \exp(-\beta E_i)]^2}{[\sum_i \exp(-\beta E_i)]^2}. \quad (5)$$

For a magnetic system like Fe_4 the ZFS pattern of the $S = 5$ ground state due to the anisotropy is described by Eq. (3) with the parameters given in Table I. Thus, C_{magn} is easily obtained from the calculated energy levels, taking into account the contributions of the three isomers. An additional factor can be introduced to best fit the experimental magnitude of the C_{magn}/R contribution: factors slightly smaller than unity account for a partial contribution of the sample to

C_{magn}/R . Fitting data below 10 K we obtain the continuous curve in Fig. 7 with $\Theta_D = 175 \pm 10$ K. It must be noted that the magnetic contribution to the specific heat is dominated by the axial parameter D , while the effect of E (at least for the values quoted in Table I) is negligible. In fact, by assuming purely axial symmetry, the zero-field energy levels of the $S = 5$ ground state are given by $E_i = D[M_i^2 - S(S+1)/3]$, with $M_i = 0, \pm 1, \pm 2, \pm 3, \pm 4, \pm 5$. If D is left as a free parameter, the best fit is obtained with $D/k_B = -0.28 \pm 0.01$ K, i.e., $B_2^0 = -8.0 \pm 0.3$ μeV . This value is in good agreement with both neutron-scattering and EPR results, which lead to an average value of -8.1 μeV for the second-order axial parameter. The larger error bar of the specific heat value is a consequence of the lower sensitivity to ZFS details of this bulk technique with respect to spectroscopies.

VI. CONCLUSIONS

From the above analysis we come to the following conclusions. The INS spectrum is consistent with the assumption of an $S = 5$ ground state with ZFS of dominant axial symmetry along the pseudo- C_3 axis perpendicular to the iron plane.^{10,12} A good fitting can be found by taking into account the intrinsic inhomogeneity of the compound, in which three isomers with different populations are present. The width of the INS transitions within the ground state, for each single isomer, is very close to the instrument resolution. For both the dominant isomers, a nonzero value of the second-order rhombic parameter E (i.e., B_2^2) is needed to interpret the INS results. The value of E obtained for the AA isomer is twice that obtained by HF-EPR in single crystals. The E/D ratios are 0.098 and 0.047 for the AA and the AB isomers, respectively. They are compatible with powder results in Ref. 10. The origin of the discrepancy between INS and HF-EPR results could be related to the fact that at the high-field values used by the last technique, the Zeeman splitting is large enough that the mixing of the ground and the first excited multiplet cannot be neglected. Due principally to the presence of different isomers, the sensitivity of the present INS experiment is not sufficient to determine the off-diagonal fourth-order contributions to the spin Hamiltonian, and therefore also to decide on the influence of negative m coefficients in the spin Hamiltonian (3). Higher-resolution and lower-energy transfer INS experiments should be needed to definitively assess this problem. Heat-capacity measurements in the low-temperature range from 2 to 10 K have been shown to be compatible with the ZFS pattern obtained by both EPR and neutron spectroscopy. Lower-temperature experiments should give better evidence for the Schottky anomaly in this compound.

¹D. Gatteschi, A. Caneschi, L. Pardi, and R. Sessoli, *Science* **265**, 1054 (1994).

²P. C. E. Stamp, *Nature (London)* **383**, 125 (1996).

³Y. Volokitin, J. Sinzig, L. J. de Jongh, G. Schmid, M. N. Vargaf-

tik, and I. I. Moiseev, *Nature (London)* **384**, 621 (1996).

⁴J. R. Friedman, M. P. Sarachik, J. Tejada, and R. Ziolo, *Phys. Rev. Lett.* **76**, 3830 (1996).

⁵W. Wernsdorfer and R. Sessoli, *Science* **284**, 133 (1999).

- ⁶R. Caciuffo, G. Amoretti, A. Murani, R. Sessoli, A. Caneschi, and D. Gatteschi, *Phys. Rev. Lett.* **81**, 4744 (1998).
- ⁷Y. Zhong, M. P. Sarachik, J. R. Friedman, R. A. Robinson, T. M. Kelley, H. Nakotte, A. C. Christianson, F. Trouw, S. M. J. Aubin, and D. N. Hendrickson, *J. Appl. Phys.* **85**, 5636 (1999).
- ⁸I. Mirebeau, M. Hennion, H. Casalta, H. Andres, H. U. Güdel, A. V. Irodova, and A. Caneschi, *Phys. Rev. Lett.* **83**, 628 (1999).
- ⁹G. Amoretti, R. Caciuffo, J. Combet, A. Murani, and A. Caneschi, *Phys. Rev. B* **62**, 3022 (2000).
- ¹⁰A. L. Barra, A. Caneschi, A. Cornia, F. Fabrizi de Biani, D. Gatteschi, C. Sangregorio, R. Sessoli, and L. Sorace, *J. Am. Chem. Soc.* **121**, 5302 (1999).
- ¹¹A. Cornia (unpublished).
- ¹²A. Bouwen, A. Caneschi, D. Gatteschi, E. Goovaerts, D. Schoemaker, L. Sorace, and M. Stefan, *J. Phys. Chem. B* **105**, 2658 (2001).
- ¹³M. T. Hutchings, *Solid State Physics*, edited by F. Seitz and D. Turnbull (Academic Press, New York, 1964).
- ¹⁴H. A. Buckmaster and Y. H. Shing, *Phys. Status Solidi A* **12**, 325 (1972).
- ¹⁵M. Affronte, J. C. Lasjaunias, and A. Corina, *Eur. Phys. J. B* **15**, 633 (2000).